Nonlinear electromagnetic response of graphene: frequency multiplication and the self-consistent-field effects

Sergey A. Mikhailov, Klaus G. Ziegler

Angaben zur Veröffentlichung / Publication details:

Mikhailov, Sergey A., and Klaus G. Ziegler. 2008. "Nonlinear electromagnetic response of graphene: frequency multiplication and the self-consistent-field effects." *Journal of Physics: Condensed Matter* 20 (38): 384204. https://doi.org/10.1088/0953-8984/20/38/384204.

Nonlinear electromagnetic response of graphene: frequency multiplication and the self-consistent-field effects

S A Mikhailov and K Ziegler

Institute for Physics, University of Augsburg, D-86135 Augsburg, Germany

E-mail: sergey.mikhailov@physik.uni-augsburg.de

Abstract

Graphene is a recently discovered carbon-based material with unique physical properties. This is a monolayer of graphite, and the two-dimensional electrons and holes in it are described by the effective Dirac equation with a vanishing effective mass. As a consequence, the electromagnetic response of graphene is predicted to be strongly nonlinear. We develop a quasi-classical kinetic theory of the nonlinear electromagnetic response of graphene, taking into account the self-consistent-field effects. The response of the system to both harmonic and pulse excitation is considered. The frequency multiplication effect, resulting from the nonlinearity of the electromagnetic response, is studied under realistic experimental conditions. The frequency upconversion efficiency is analyzed as a function of the applied electric field and parameters of the samples. Possible applications of graphene in terahertz electronics are discussed.

1. Introduction

The region of the electromagnetic spectrum from 0.3 to 20 THz (the so called terahertz gap) is a frontier area for research in physics, chemistry, biology, material science and medicine [1]. Due to the recent progress in THz technology [1–3], the THz studies continue to expand, involving more and more scientists in the development of new sources and detectors of THz radiation, as well as in research on applications of THz waves in different areas. The search for new methods of THz emission and detection and development of simple, compact and inexpensive THz sources and detectors remains a challenging problem.

The most common technique for producing low-power electromagnetic radiation at frequencies above 0.3 THz is through nonlinear multiplication (upconversion) of lower frequency oscillators [3, 4], $\Omega \to m\Omega$, $m = 2, 3, \ldots$. Such upconverters, which are commonly based on GaAs Schottky barrier diodes, successfully work as doublers and triplers ($m = 2$ and 3), but provide very poor conversion efficiency for higher order harmonics ($m > 3$) [3, 4]. The search for alternative nonlinear materials, which could provide efficient frequency multiplication, especially with an upconversion factor $m > 3$, is therefore highly desirable.

In this paper we discuss the recently predicted [5] effect of the frequency multiplication in graphene. Graphene is a new material, which was experimentally obtained about three years ago [6–8] and immediately attracted great interest from researchers; for recent reviews see [9, 10]. Graphene is a monolayer of graphite, in which carbon atoms are packed in a dense two-dimensional (2D) honeycomb lattice [11, 12]. This is a two-dimensional semimetal, with a very specific electronic band structure, figure 1. The lower ($l = 1$) and upper ($l = 2$) branches of the energy spectrum $E_{\mathbf{p}l}$ touch each other at six points at the corners of the hexagon-shaped Brillouin zone. In the ideal case of a uniform, undoped graphene at zero temperature, the lower band $E_{\mathbf{p}1}$ is fully occupied while the upper band $E_{\mathbf{p}2}$ is empty, and the Fermi level goes through these six, so called Dirac points $\mathbf{P}^{(i)} = \hbar\mathbf{K}^{(i)}$, $i = 1, \ldots, 6$. Near the Dirac points, at $\mathbf{p} \approx \hbar\mathbf{K}^{(i)}$, the electrons in graphene have a linear, quasirelativistic dispersion with zero effective mass of quasiparticles [9],

$$E_{\mathbf{p}l} = (-1)^l V|\mathbf{p} - \hbar\mathbf{K}^{(i)}| = (-1)^l V\sqrt{\tilde{p}_x^2 + \tilde{p}_y^2}, \qquad (1)$$

where $\tilde{\mathbf{p}} = \mathbf{p} - \hbar\mathbf{K}^{(i)}$. Only two of the six Dirac points in the Brillouin zone, usually referred to as K and K' points, are inequivalent [11, 12, 14]. In the phenomena,

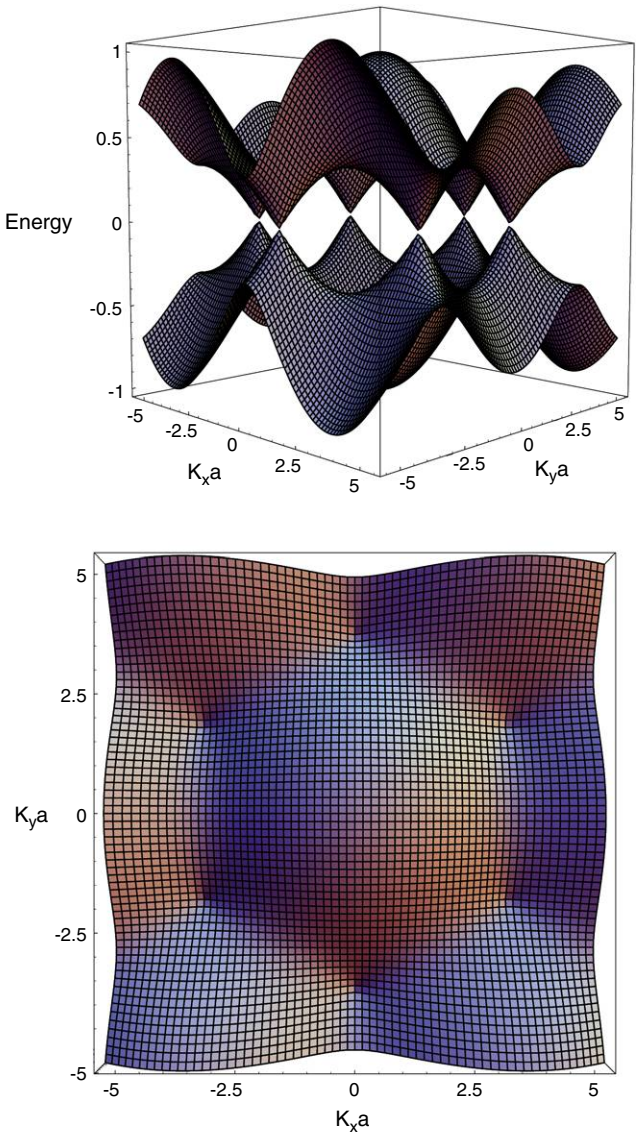

Figure 1. The band structure of electrons in graphene (side view and top view), calculated in the tight-binding approximation. The energy is normalized to the full width of the energy band $\Delta E = 2\sqrt{3}\hbar V/a$, where $V \approx 10^8$ cm s^{-1} is the Fermi velocity, equation (1), and $a = 2.46$ Å is the lattice constant. The two branches of the energy spectrum $E_{\mathbf{p}l}$, $l = 1, 2$, touch each other at six points at corners of the hexagonal Brillouin zone. The coordinates of the Dirac points are $\mathbf{K}_i = (4\pi/3a)(\cos\phi_i, \sin\phi_i)$, where $\phi_i = \pi/6 + 2\pi i/3$, $i = 1, \ldots, 6$. Details of the band structure of graphene and of the tight-binding calculations can be found, e.g., in [11–13].

discussed here, the states of the K and K' cones give additive contributions to the ac graphene response, so that one can consider only the states in the vicinity of one Dirac cone, accounting for the second cone by introducing the valley-degeneracy factor $g_v = 2$. The velocity V in (1) is about 10^8 cm s^{-1}, according to measurements [7, 8]. Near the $\mathbf{K}^{(i)}$ points the graphene quasiparticles are described by two-component spinor wavefunctions, determined by the effective Dirac equation, and are called Dirac fermions.

The unusual, linear dispersion of graphene quasiparticles near the Fermi level leads to a number of interesting and so far not fully understood transport phenomena, such as minimal electrical conductivity [7, 8, 15–26], absence of weak localization [27], unconventional quantum Hall effect [7, 8, 16, 28–30], observable even at room temperature [31], and others. Electrodynamic properties of graphene, which have been studied both experimentally [32–39] and theoretically [5, 16, 17, 25, 29, 30, 40–53], also demonstrate non-trivial features in the frequency-dependent conductivity [16, 25, 29, 40, 53], photon-assisted transport [41], microwave and far-infrared response [30, 42–46], plasmon spectrum [47–51], etc. New electromagnetic modes, specific only for the graphene system, have been also predicted [52, 53].

Both the transport and electrodynamic properties, briefly outlined above, have been studied within the linear-response theory. Going beyond the linear-response approach, one can show [5, 54] that graphene should demonstrate *strongly nonlinear* electromagnetic response at relatively low amplitudes of the external electric field. In particular, irradiation of graphene by an electromagnetic wave with the frequency Ω should lead to the frequency multiplication $\Omega \to m\Omega$ with odd values of $m = 3, 5, 7, \ldots$. This makes graphene a simple and natural frequency multiplier [5, 54] and opens up exciting opportunities for using graphene in terahertz electronics.

In general, prospects for building graphene-based devices for terahertz applications are very attractive. Apart from the frequency multiplication, graphene devices could be used in *plasmon*-based voltage-controlled sources and detectors of THz radiation. The physics of such devices has long been discussed in the literature [55–60] and the main ideas of 2D plasmon-assisted detection and generation of radiation have been confirmed in a number of experiments on conventional 2D electron systems [61–64]. Graphene has that advantage that the Fermi velocity of electrons in it is much higher than in other semiconductor materials, and its plasma frequency is widely tunable and lies in the THz range [50, 51]. It should be noticed that a material closely related to graphene—carbon nanotubes—has also demonstrated a great potential for terahertz applications [65–72].

In this paper we discuss the effects of the nonlinear electromagnetic response and the frequency multiplication in graphene [5, 54]. We consider the response of graphene to a strong uniform external time-dependent electric field within the semi-classical kinetic theory (section 2). In addition to results obtained in [5, 54], we take into account the self-consistent-field effects (section 2.3), which should be important under realistic experimental conditions, and discuss both harmonic (section 2) and pulse excitation (section 3) of the system. The results obtained are summarized and discussed in section 4.

2. Self-consistent kinetic theory of nonlinear electromagnetic response of graphene

2.1. Qualitative consideration

Due to the linear dispersion (1), the response of graphene to an external electromagnetic field turns out to be

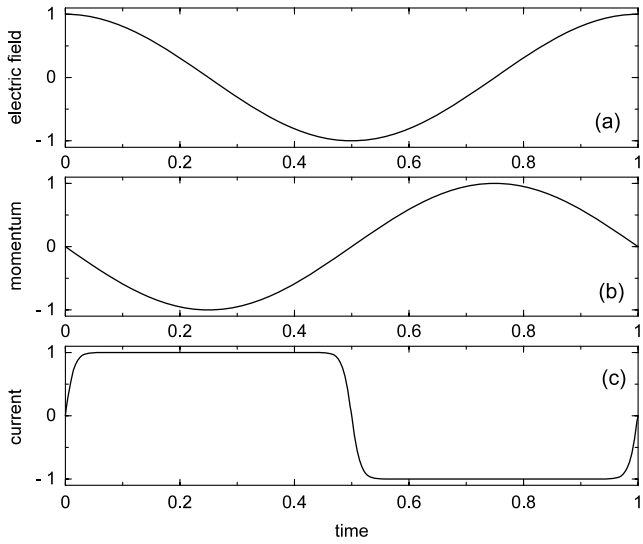

Figure 2. Qualitative behavior of time dependences of (a) the electric field, (b) the momentum, and (c) the velocity and current of a particle with the energy dispersion (2).

intrinsically nonlinear, which naturally leads to the frequency multiplication effect. Physically, the possibility of the frequency upconversion in graphene can be explained in a very simple manner. Consider a classical 2D particle with the charge $-e$ and the energy spectrum

$$E_{\mathbf{p}2} = Vp = V\sqrt{p_x^2 + p_y^2} \tag{2}$$

in the external time-dependent harmonic electric field $E_x(t) = E_0 \cos \Omega t$, figure 2(a). From now on we will consider only electrons in the vicinity of one Dirac cone, omit the tilde in (1) and take into account the presence of two inequivalent cones in the Brillouin zone by the valley-degeneracy factor $g_\mathrm{v} = 2$. According to the Newton equation of motion $\mathrm{d}p_x/\mathrm{d}t = -eE_x(t)$, the momentum $p_x(t)$ is then given by the sine function $p_x(t) \equiv p_0(t) = -(eE_0/\Omega)\sin \Omega t$, figure 2(b). In conventional 2D electron systems with the parabolic energy dispersion, the velocity v_x and hence the current $j_x = -en_s v_x$ are proportional to p_x, so that the normal 2D system responds at the same frequency Ω (here n_s is the areal density of particles). In graphene, however, the velocity

$$v_x = \frac{\partial E_{\mathbf{p}2}}{\partial p_x} = V\frac{p_x}{\sqrt{p_x^2 + p_y^2}} \tag{3}$$

is a strongly nonlinear function of p_x, therefore the response of graphene is substantially anharmonic, figure 2(c). In the extreme limit, when p_y in equation (3) is close to zero, v_x is proportional to $\mathrm{sgn}(p_x)$ and the ac electric current is

$$j_x(t) = en_s V\,\mathrm{sgn}(\sin \Omega t)$$
$$= en_s V\frac{4}{\pi}\left\{\sin \Omega t + \frac{1}{3}\sin 3\Omega t + \frac{1}{5}\sin 5\Omega t + \ldots\right\}. \tag{4}$$

The current (4) contains all odd Fourier harmonics, with the amplitudes j_m, $m = 1, 3, 5\ldots$, falling very slowly with the harmonic number, $j_m \sim 1/|m|$. An isolated graphene layer should thus work as a simple and natural frequency multiplier, with the operating frequency variable in a broad range.

2.2. Kinetic approach

The current (4) above is independent of the electric field, which means that equation (4) is not completely correct. The reason is that in the above simple consideration we did not take into account the Fermi distribution of electrons over the quantum states in graphene. To do this, we use [5] the kinetic Boltzmann theory, which allows one to get an exact response of the system, not imposing any restrictions on the amplitude of the external electric field $\mathbf{E}^{\mathrm{ext}}(t)$.

In a real experimental situation, the graphene sheet lies on top of a silicon oxide–silicon structure, and the gate voltage V_G can be applied between graphene and the silicon substrate, in order to control the density of electrons or holes in graphene. In addition, the graphene–SiO_2–Si system can be doped by impurities. Both the gate voltage and the doping can shift the chemical potential μ of electrons in graphene to the upper $E_{\mathbf{p}2}$ or to the lower $E_{\mathbf{p}1}$ band. Assume that the chemical potential μ lies in the upper band $E_{\mathbf{p}2} = Vp$, the temperature is small, $T \ll \mu$, and the system is subjected to the external time-dependent ac electric field $\mathbf{E}^{\mathrm{ext}}(t)$. Then the momentum distribution function of electrons $f_\mathbf{p}(t)$ is described by the Boltzmann equation

$$\frac{\partial f_\mathbf{p}(t)}{\partial t} - \frac{\partial f_\mathbf{p}(t)}{\partial \mathbf{p}} e\mathbf{E}^{\mathrm{ext}}(t) = 0, \tag{5}$$

in which we have ignored collisions of electrons with impurities, phonons and other lattice imperfections. Equation (5) has the exact solution

$$f_\mathbf{p}(t) = \mathcal{F}_0\left(\mathbf{p} - \mathbf{p}_0(t)\right), \tag{6}$$

where $\mathcal{F}_0(\mathbf{p}) = \{1 + \exp[(Vp - \mu)/T]\}^{-1}$ is the Fermi–Dirac function, and $\mathbf{p}_0(t) = -e\int_{-\infty}^{t}\mathbf{E}^{\mathrm{ext}}(t')\,\mathrm{d}t'$ is the solution of the single particle classical equation of motion. The electric current $\mathbf{j}(t) = -eg_\mathrm{s}g_\mathrm{v}S^{-1}\sum_\mathbf{p}\mathbf{v}f_\mathbf{p}(t)$ then assumes the form

$$\mathbf{j}(t) = -\frac{g_\mathrm{s}g_\mathrm{v}eV}{(2\pi\hbar)^2}\int\frac{\mathbf{p}\,\mathrm{d}\mathbf{p}}{p}\mathcal{F}_0\left(\mathbf{p} - \mathbf{p}_0(t)\right), \tag{7}$$

where $g_\mathrm{s} = 2$ is the spin degeneracy and S is the sample area. If the temperature is zero, $T = 0$, and the chemical potential is finite, $\mu > 0$, the current $\mathbf{j}(t)$ can be rewritten in the form

$$\frac{\mathbf{j}(t)}{en_sV} = \frac{\mathbf{P}}{\sqrt{1 + P^2}}\mathcal{G}(Q), \tag{8}$$

where $\mathbf{P} \equiv \mathbf{P}(t) = -\mathbf{p}_0(t)/p_\mathrm{F}$, $P(t) = |\mathbf{P}(t)|$, $p_\mathrm{F} = \mu/V$ is the Fermi momentum, and

$$n_s \equiv n_\mathrm{e} = \frac{g_\mathrm{s}g_\mathrm{v}p_\mathrm{F}^2}{4\pi\hbar^2} = \frac{g_\mathrm{s}g_\mathrm{v}\mu^2}{4\pi\hbar^2V^2} \tag{9}$$

is the density of electrons in the upper band. The function $\mathcal{G}(Q)$ in (8) is defined and analyzed in appendix, and $Q(t) \equiv 2P(t)/[1 + P^2(t)] \leqslant 1$.

If the external field $\mathbf{E}^{\mathrm{ext}}$ is small, so that the Fermi distribution is weakly disturbed, $P(t) \ll 1$, the function $G(Q) \approx 1$, see equation (A.3), and $\mathbf{j}(t) \approx (n_se^2V/p_\mathrm{F})\int_{-\infty}^{t}\mathbf{E}^{\mathrm{ext}}(t')\,\mathrm{d}t'$. In this, *linear-response* regime,

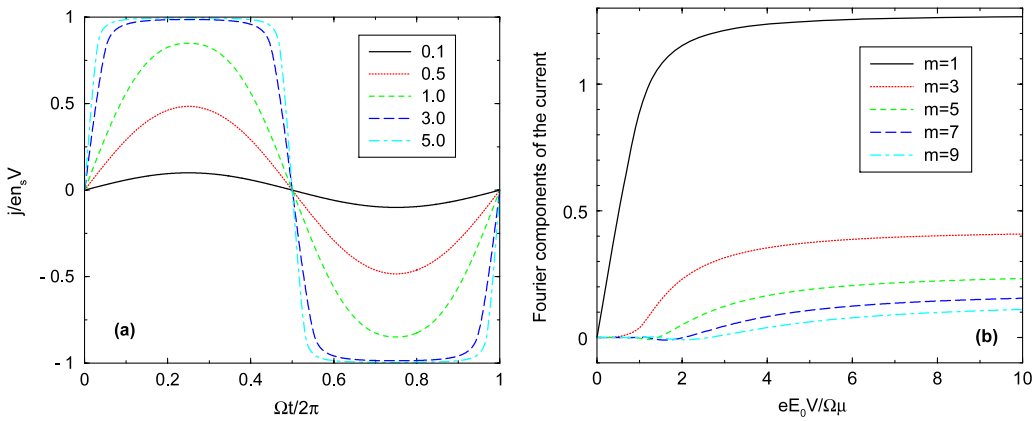

Figure 3. (a) The time dependence of the ac electric current, measured in units en_sV, at harmonic excitation of the system at the frequency Ω. The temperature is zero, $T/\mu = 0$; the curves are labeled by the values of the electric field parameter $\mathcal{E} = eE_0V/\Omega\mu$. (b) The Fourier components of the current (8) as a function of $\mathcal{E}$ at $T/\mu = 0$. At $\mathcal{E}_T \to \infty$ the curves tend to the values $4/\pi m$; see equation (4).

the current is directly proportional to the electric field. If the external excitation is harmonic,

$$\mathbf{E}^{\rm ext}(t) = \mathbf{E}_0 \cos \Omega t, \tag{10}$$

the current is $\mathbf{j}(t) \approx (n_s e^2 V/p_{\rm F}\Omega)\mathbf{E}_0 \sin \Omega t$, which corresponds to the linear-response frequency-dependent collisionless scalar Drude conductivity [25, 29, 30, 42, 43, 53]

$$\sigma(\Omega) = \frac{{\rm i}n_s e^2 V}{\Omega p_{\rm F}} = {\rm i}\frac{e^2}{\hbar}\frac{g_{\rm s}g_{\rm v}}{4\pi}\frac{\mu}{\hbar\Omega}. \tag{11}$$

If the external field $\mathbf{E}^{\rm ext}$ is large and the Fermi distribution is strongly disturbed, $P(t)$ can be much larger than unity, the function $\mathcal{G}(Q) \approx 1$, and the response of the system to a harmonic excitation (10) is described by equation (4). The nonlinear regime (4) is thus achieved at $|p_0| \gg p_{\rm F}$, or at

$$\mathcal{E} \equiv \frac{eE_0V}{\Omega\mu} \gg 1 : \tag{12}$$

the energy gained by electrons from the external field during the oscillation period should be large as compared to their average equilibrium (Fermi) energy.

Figure 3(a) illustrates the time dependence of the current (8) at the harmonic excitation of the system (10). One sees that in the low-field limit the response is linear (the $j(t)$ dependence has a sinusoidal shape), while at strong fields the time dependence of the current tends to that given by equation (4). In figure 3(b) we show the Fourier components of the current versus the field parameter $\mathcal{E}$. One sees that when $\mathcal{E}$ becomes larger than $\simeq 4$, the Fourier amplitudes saturate and one enters the ultimate nonlinear regime.

The strong-field condition (12) can be rewritten as

$$E_0 \gg \frac{2\hbar\Omega\sqrt{\pi n_s}}{e\sqrt{g_{\rm s}g_{\rm v}}}, \tag{13}$$

which shows that the required ac electric field grows linearly with the electromagnetic wave frequency and with the square root of the electron density. At $f \simeq 100$ GHz and $n_s \simeq 10^{11}$ cm^{-2}, the inequality (13) is fulfilled at $E_0 \gtrsim 200$ V cm^{-1}.

The results obtained above refer to the case $T/\mu = 0$ (μ is finite). The opposite limit $\mu = 0$ (at a finite temperature, $\mu/T = 0$) is difficult to realize in the whole sample, at least in currently available systems. Due to the inhomogeneity of the samples, the zero-energy point fluctuates in space, with a typical local electron or hole density of the order of 10^{11} cm^{-2} [73]. The condition $\mu/T = 0$ can thus be satisfied only locally, at certain points inside the sample. Nevertheless, for the sake of completeness (and in view of possible availability of higher quality samples in future), we also present here results [5] for the case $\mu/T = 0$. For arbitrary values of μ/T some results can be also found in [54].

At a finite temperature and the vanishing chemical potential $\mu = 0$ both electrons and holes contribute to the charge carrier density $n_s = n_{\rm e} + n_{\rm h} = \pi g_{\rm s}g_{\rm v}T^2/12\hbar^2V^2$ and to the current. Starting again from equation (7) but accounting for the hole contribution and setting $\mu = 0$, we get

$$\mathbf{j}(t) = en_sV\frac{\mathbf{P}_T}{P_T}\frac{12}{\pi^3}\int_0^\infty x\,{\rm d}x \times \int_0^\pi {\rm d}\theta \frac{\cos\theta}{1+\exp\left(\sqrt{x^2+P_T^2-2xP_T\cos\theta}\right)}, \tag{14}$$

where the momentum $\mathbf{p}_0(t)$ is now normalized by the characteristic temperature-dependent momentum, $\mathbf{P}_T \equiv \mathbf{P}_T(t) = -\mathbf{p}_0(t)/p_T$, $P_T(t) = |\mathbf{P}_T(t)|$, and $p_T = T/V$.

If the external field is small, $P_T(t) \ll 1$, equation (14) gives the linear-response current

$$\mathbf{j}(t) \approx en_sV\mathbf{P}_T(t)\frac{6\ln 2}{\pi^2} = \frac{n_se^2V^2}{T}\frac{6\ln 2}{\pi^2}\int_{-\infty}^t \mathbf{E}^{\rm ext}(t')\,{\rm d}t', \tag{15}$$

proportional to the electric field. If the external excitation is harmonic, equation (10), the current is $\mathbf{j}(t) = (n_se^2V^2/T\Omega)(6\ln 2/\pi^2)\mathbf{E}_0\sin\Omega t$, which corresponds to the linear-response frequency-dependent collisionless Drude conductivity [25]

$$\sigma_{\mu=0,T}(\Omega) = \frac{6\ln 2}{\pi^2}\frac{{\rm i}n_se^2V^2}{T\Omega} = {\rm i}\frac{\ln 2}{2\pi}\frac{e^2}{\hbar}\frac{g_{\rm s}g_{\rm v}T}{\hbar\Omega}. \tag{16}$$

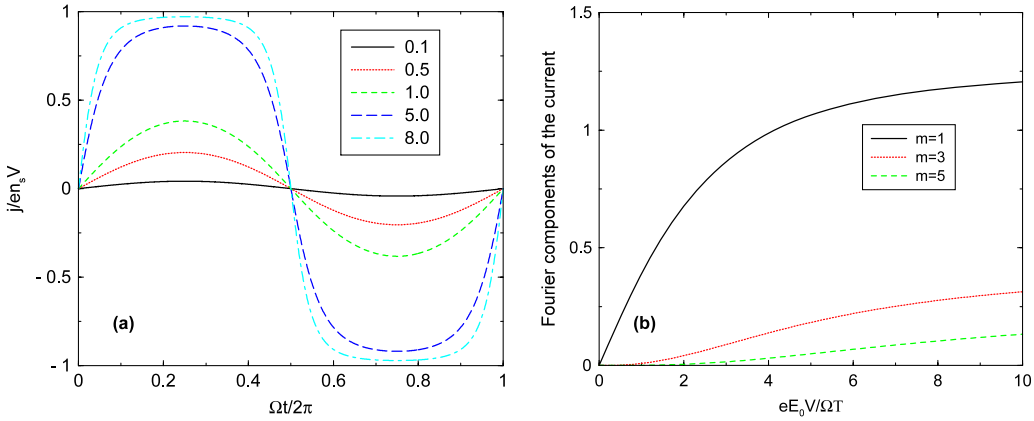

Figure 4. (a) The time dependence of the ac electric current, measured in units en_sV, at harmonic excitation of the system at the frequency Ω. The chemical potential is zero and the temperature is finite, $\mu/T = 0$; the curves are labeled by the values of the electric field parameter $\mathcal{E}_T = eE_0V/\Omega T$. (b) The Fourier components of the current (14) as a function of the field parameter $\mathcal{E}_T = eE_0V/\Omega T$ at $\mu/T = 0$. At $\mathcal{E}_T \to \infty$ the curves tend to the values $4/\pi m$; see equation (4).

In the strong-field regime $P_{T0} \gtrsim 1$ equation (14) is reduced, again, to (4). The dimensionless field parameter in the case $\mu/T = 0$ is defined as $\mathcal{E}_T = eE_0V/T\Omega$.

Figure 4(a) demonstrates the time dependence of the current (14) at the harmonic excitation of the system (10). The $j(t)$ dependence is qualitatively similar to that shown in figure 3(a). In figure 4(b) we show the Fourier components of the ac electric current, for $m = 1$, 3 and 5, as a function of the field parameter $\mathcal{E}_T$ at $\mu = 0$.

In the case $\mu/T = 0$ the strong-field condition $\mathcal{E} \gtrsim 1$ assumes the form

$$E_0 \gtrsim \frac{\Omega T}{eV}. \tag{17}$$

At the temperature $T \simeq 100$ K and the frequency $f \simeq 100$ GHz this corresponds to the requirement $E_0 \gtrsim 50$ V cm^{-1}.

Using the quasi-classical (Boltzmann) approach for the description of electromagnetic response of graphene imposes certain restrictions on the validity of the presented theory. Physically, using the Boltzmann theory, one takes into account the intra-band contribution to the ac electric current, but ignores the inter-band contribution due to transitions between the lower (quasi-hole) and the upper (quasi-electron) bands. This is possible if the frequency of the external radiation satisfies the inequality $\hbar\Omega \ll \max\{\mu, T\}$. In practically interesting cases (the density $n_s \simeq 10^{11}$–10^{12} cm^{-2}, room temperature) this restricts the frequency of radiation by ∼10–30 THz. The presented quasi-classical theory can thus be used in the whole terahertz gap.

2.3. Self-consistent-field effects and radiative decay

In section 2.2 we have not considered effects of the radiative decay, which can be important under realistic experimental conditions in graphene. It was assumed that the graphene electrons move in the sample under the action of the external electric field $\mathbf{E}^{\rm ext}(t)$, and this directly leads to the time-dependent electric current $\mathbf{j}(t)$, equation (8). In general, however, the time-dependent electric current creates, in its turn, a secondary (induced) electric field $\mathbf{E}^{\rm ind}(t)$, which acts back on the electrons and should be added to the external field. Calculating the response of the system, one should take into account that electrons respond not to the external, but to the total self-consistent electric field $\mathbf{E}^{\rm tot}(t) = \mathbf{E}^{\rm ext}(t) + \mathbf{E}^{\rm ind}(t)$. This results in the effect of electromagnetic reaction of the medium (graphene) to the external field and can reduce the frequency upconversion efficiency. How substantially the radiative decay suppresses the efficiency of the frequency multiplication is studied below.

Consider an infinite 2D electron system with the graphene sheet lying in the plane $z = 0$. We assume that the external electromagnetic wave is incident upon the graphene layer along the z axis and induces the ac current in the layer. This current produces the induced electric field $\mathbf{E}^{\rm ind}(t)$, which is added to the external one. The Boltzmann equation for the momentum distribution function of the electrons should then be written as

$$\frac{\partial f_{\mathbf{p}}(t)}{\partial t} - \frac{\partial f_{\mathbf{p}}(t)}{\partial \mathbf{p}} e\mathbf{E}^{\rm tot}_{z=0}(t) = 0, \tag{18}$$

instead of (5). The solution of this equation, as well as the electric current, can again be written in the form (6) and (7), respectively, but the classical momentum $\mathbf{p}_0(t)$ now satisfies the equation

$$\begin{aligned}\mathbf{p}_0(t) &= -e\int_{-\infty}^{t} \mathbf{E}^{\rm tot}_{z=0}(t')\,{\rm d}t' \\ &= -e\int_{-\infty}^{t} \left[\mathbf{E}^{\rm ind}_{z=0}(t') + \mathbf{E}^{\rm ext}_{z=0}(t')\right]{\rm d}t',\end{aligned} \tag{19}$$

where the field $\mathbf{E}^{\rm tot}_{z=0}(t)$ is not known and should be calculated self-consistently. To do this, we recall that the current and the induced electric field are related by the Maxwell equations,

$$\mathbf{E}^{\rm ind}_{z=0}(t) = -2\pi\mathbf{j}(t)/c. \tag{20}$$

Combining (19), (20) and (7) we get the following self-consistent equation of motion for the momentum $\mathbf{p}_0(t)$:

$$\frac{{\rm d}\mathbf{p}_0(t)}{{\rm d}t} + \frac{e^2 g_s g_v V}{2\pi\hbar^2 c}\int \frac{\mathbf{p}\,{\rm d}\mathbf{p}}{p}\mathcal{F}_0\left(\mathbf{p} - \mathbf{p}_0(t)\right) = -e\mathbf{E}^{\rm ext}_{z=0}(t). \tag{21}$$

After the nonlinear equation (21) is resolved with respect to the momentum $\mathbf{p}_0(t)$, the current $\mathbf{j}(t)$ can be found from equation (7). Equations (21) and (7) describe the nonlinear self-consistent response of graphene to an arbitrary external time-dependent electric field $\mathbf{E}^{\rm ext}_{z=0}(t)$. The second term in the left-hand side of equation (21) describes the radiative decay effects in the infinite 2D graphene layer.

In conventional 2D electron systems with the parabolic energy dispersion and the effective mass $m^\star$ of 2D electrons the self-consistent equations for $\mathbf{p}_0(t)$ and $\mathbf{j}(t)$, similar to (21) and (7), have the form

$$\frac{{\rm d}\mathbf{p}_0(t)}{{\rm d}t} + \frac{2\pi n_s e^2}{m^\star c}\mathbf{p}_0(t) = -e\mathbf{E}^{\rm ext}_{z=0}(t), \qquad \mathbf{j}(t) = -\frac{en_s}{m^\star}\mathbf{p}_0(t). \tag{22}$$

Here $\Gamma_{\rm par} \equiv 2\pi n_s e^2/m^\star c$ is the radiative decay rate [74] in the conventional (parabolic) 2D electron systems. In (22) we have ignored the scattering due to impurities and phonons (the corresponding term $\gamma\mathbf{p}_0(t)$ can be added to the left-hand side of the first equation (22)). In high-electron-mobility GaAs/AlGaAs quantum-well samples the radiative decay $\Gamma_{\rm par}$ substantially exceeds the scattering rate γ, $\Gamma_{\rm par} \gg \gamma$, and determines the linewidth of the cyclotron, plasmon, and magnetoplasmon resonances [74, 75]. As the graphene mobility is also very high, one can expect that at high frequencies the radiative effects are more important in graphene than the scattering effects. This justifies ignoring the scattering terms in equation (21).

Returning back to the non-parabolic graphene system, we rewrite (21) (at $T = 0$) in terms of the dimensionless momentum $\mathbf{P}(t) = -\mathbf{p}_0(t)/p_{\rm F}$:

$$\frac{{\rm d}\mathbf{P}(t)}{{\rm d}t} + \Gamma\frac{\mathbf{P}}{\sqrt{1+P^2}}\mathcal{G}(Q) = \frac{e}{p_{\rm F}}\mathbf{E}^{\rm ext}_{z=0}(t), \tag{23}$$

where

$$\Gamma = \frac{g_s g_v}{4}\frac{e^2}{\hbar c}\frac{2\mu}{\hbar} = V\frac{e^2}{\hbar c}\sqrt{g_s g_v \pi n_s}. \tag{24}$$

The current is determined, again, by equation (8).

In the linear-response regime, when $|P| \ll 1$ and $\mathcal{G} \approx 1$, equation (23) gives

$$\frac{{\rm d}\mathbf{P}(t)}{{\rm d}t} + \Gamma\mathbf{P}(t) = \frac{e}{p_{\rm F}}\mathbf{E}^{\rm ext}_{z=0}(t). \tag{25}$$

From here one sees that the quantity Γ has the physical meaning of the radiative decay rate in graphene *in the linear-response regime*. In contrast to $\Gamma_{\rm par}$, Γ is proportional to the square root of the charge carrier density. For experimentally relevant densities n_s the value of Γ lies in the subterahertz range, $\Gamma/2\pi\,({\rm THz}) \approx 0.13\sqrt{n_s(10^{11}\ {\rm cm}^{-2})}$.

Now consider the response of graphene to a harmonic excitation (10). The solution now depends on two dimensionless parameters, $\mathcal{E} = eE_0V/\mu\Omega$ and Γ/Ω. If the field parameter $\mathcal{E}$ is small, $|P| \ll 1$, $\mathcal{G} \approx 1$, and the response is linear. The strong-electric-field results for the time dependence of the momentum $P(t)$ and of the dimensionless electric current $j(t)/en_sV$ are shown in figure 5. If Γ/Ω does not exceed the value of about $\mathcal{E}/2$ (=5 in the example of figure 5), the self-consistent-field effects lead only to the phase shift of the current, not influencing the shape of the current–time curves and hence not reducing the amplitudes of the higher harmonics. At higher values of Γ/Ω (between $\Gamma/\Omega \sim \mathcal{E}/2$ and $\Gamma/\Omega \sim \mathcal{E}$) the shape of the current–time curves smoothly modifies from the step-like form to the sinusoidal form, and at $\Gamma/\Omega \gtrsim \mathcal{E}$ the higher harmonics are fully suppressed. Quantitatively, this can be seen from analysis of the Fourier harmonics of the current. Expanding the current in the Fourier series $j(t)/en_sV = \sum_m [A_m\cos(m\Omega t) + B_m\sin(m\Omega t)]$, we calculate the amplitudes $F_m = \sqrt{A_m^2 + B_m^2}$ and plot them as a function of Γ/Ω in figure 6 for the lowest harmonic numbers from 1 to 9. One sees that, indeed, the higher harmonics are suppressed at $\Gamma/\Omega \gtrsim \mathcal{E}$, but almost not influenced by the radiative decay if $\Gamma/\Omega \lesssim 0.7\mathcal{E}$. We have performed similar calculations at other values of the field parameter $\mathcal{E}$ and found the same results if $\mathcal{E} \gg 1$.

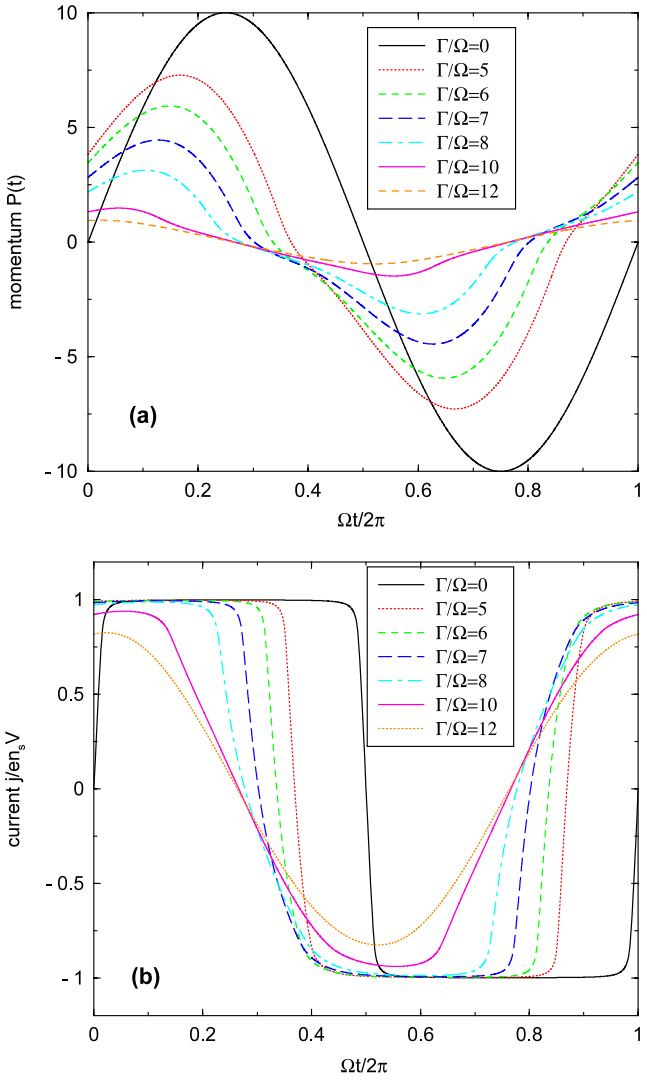

Figure 5. The time dependence of (a) the momentum $P(t)$ and (b) the current $j(t)/en_sV$ at the field parameter $\mathcal{E} = 10$ at several values of the radiative decay Γ/Ω.

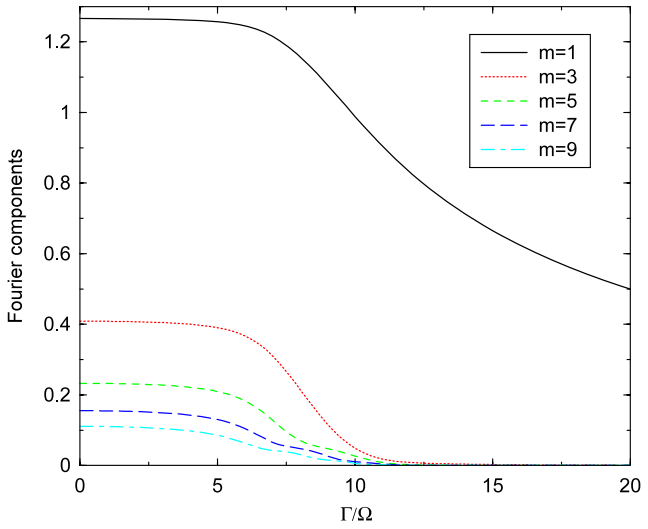

Figure 6. Fourier harmonics of the current $j(t)/en_sV$ at $\mathcal{E} = 10$ as a function of Γ/Ω.

The condition of the efficient frequency upconversion, with account of the self-consistent-field effects and of the radiative decay, thus assumes the form $\mathcal{E} \gtrsim \Gamma/\Omega$, or

$$E_0 \gtrsim \frac{\mu\Gamma}{eV} = \frac{2\pi n_s eV}{c} \approx 300\ \mathrm{V\ cm^{-1}} \times n_s\ (10^{11}\ \mathrm{cm^{-2}}). \tag{26}$$

This condition does not depend on the frequency of radiation.

It should be noticed that in the above consideration the sample was assumed to be infinite. Quantitatively, this means that the lateral dimensions of the graphene layer L should exceed the wavelength of radiation λ. At the frequency of 1 THz the above derived formulas will thus be valid for samples with dimensions larger than $\simeq$300 μm. As the currently available samples are smaller ($\simeq$10–30 μm), the above consideration overestimates the role of the radiative decay. If $L \lesssim \lambda$, the radiative decay rate Γ in the above formulas should be replaced by $\Gamma(L/\lambda)^2$, [75]. The upconversion effect should then be observed at electric fields lower than those given by the estimate (26).

3. Response of graphene to a pulse excitation

Now consider the response of graphene to a pulse excitation $\mathbf{E}^{\mathrm{ext}}(t) = \mathbf{E}_0\tau_0\delta(t)$, where $\mathbf{E}_0$ and τ_0 are the amplitude and the duration of the pulse. The pulse amplitude $\mathbf{E}_0$ can be arbitrarily strong. Equation (23) now assumes the form

$$\frac{\mathrm{d}\mathbf{P}(t)}{\mathrm{d}t} + \Gamma\frac{\mathbf{P}}{\sqrt{1+P^2}}\mathcal{G}(Q) = \frac{e}{p_{\mathrm{F}}}\mathbf{E}_0\tau_0\delta(t) \tag{27}$$

and can be solved explicitly; see appendix (the current is determined again by equation (8)). Figure 7(a) shows the dependence $P(t)$, calculated from equation (A.5), at different values of the electric field parameter $P_0 = eE_0\tau_0/p_{\mathrm{F}}$. If the external field is small, $P_0 \ll 1$, the system relaxes after the pulse excitation exponentially, similar to the conventional 2D electron systems with the parabolic dispersion,

$$P(t) = P_0\exp(-\Gamma t), \qquad P_0 \lesssim 1. \tag{28}$$

The characteristic decay time is determined in this case by the inverse radiation decay rate (24). If the external field is strong, $P_0 \gg 1$, the momentum of the system first decays linearly in time,

$$P(t) = P_0 - \Gamma t, \qquad P_0 \gtrsim 1. \tag{29}$$

The linear dependence (29) remains valid until $P(t)$ reduces to $P(t) \simeq 1$ (until $t \simeq P_0/\Gamma$); after this $P(t)$ decays exponentially as in (28). The current $\mathbf{j}(t)$ in the strong excitation regime $P_0 \gg 1$ reaches its highest possible value en_sV and is time independent at $t \lesssim P_0/\Gamma$, and then exponentially decays (at the timescale $\simeq \Gamma^{-1}$) down to zero, as shown in figure 7(b).

The fact that after the pulse excitation electrons in graphene move with a constant velocity $V \approx 10^8$ cm s^{-1} for quite a long time, $\sim P_0/\Gamma$, may have interesting applications. In a finite-size graphene sample such excited electrons will be reflected by the boundaries and oscillate in the sample with the typical frequency $\sim V/L$, lying in the terahertz range, if the sample dimension $L \lesssim 1$ μm. As at $P_0 \gg 1$ the time P_0/Γ is much longer than the oscillation period, this may lead to a coherent terahertz radiation from graphene excited by a strong pulse electric field. In order to properly describe this phenomenon the plasma effects should be taken into account.

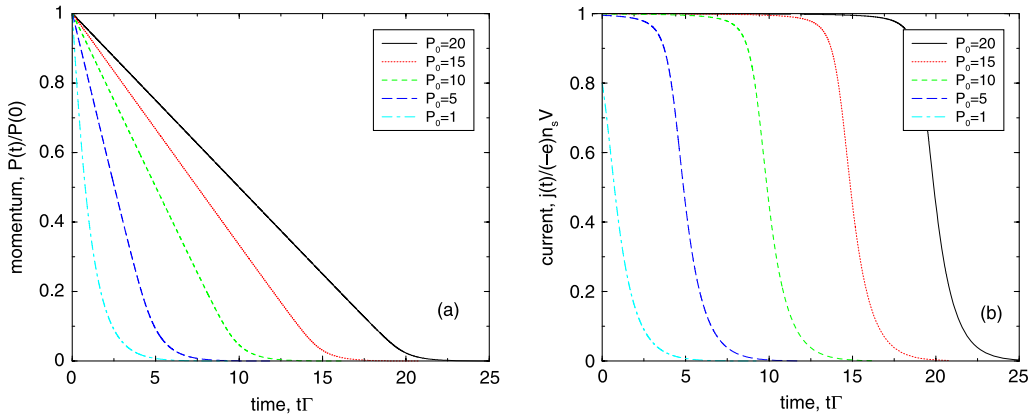

Figure 7. The time dependence of (a) the momentum $P(t)/P_0$ and (b) the electric current $j(t)/en_sV$, at a pulse excitation of graphene. Different curves correspond to different pulse amplitudes $P_0 = eE_0\tau_0/p_{\mathrm{F}}$.

4. Summary and conclusions

We have developed the quasi-classical kinetic theory of the nonlinear electromagnetic response of graphene. Electrodynamic equations, describing the self-consistent response of the system to a uniform time-dependent external electric field, have been derived and solved for the cases of harmonic and pulse excitation. The presented theory is valid at $\hbar\Omega \lesssim \max\{\mu, T\}$, which covers the frequency range up to ∼10–30 THz for relevant experimental conditions.

If the system is subjected to a pulse excitation and the amplitude of the external field is small (the linear regime), its response is described by a standard exponential decay with the characteristic decay rate Γ. The density dependence of the radiative decay rate in graphene ($\Gamma \propto n_s^{1/2}$) differs from that of conventional 2D electron systems ($\Gamma_{\rm par} \propto n_s$). In the nonlinear regime, when the pulse amplitude is strong, the response of the system is not exponential. The average momentum of graphene electrons falls linearly after the pulse excitation, with the average current remaining constant during a time proportional to the amplitude of the external field and inversely proportional to Γ.

The graphene layer excited by the harmonic electromagnetic wave with the frequency Ω, re-emits radiation at higher harmonics $m\Omega$, $m = 3, 5, 7, \ldots$, with the efficiency falling slowly, as $1/|m|$. The amplitude of the external electric field required for getting into the nonlinear regime grows with the charge carrier density and is of the order of several hundred V cm^{-1} for typical experimental parameters. The operating frequency of such a frequency multiplier can vary in a broad range, from microwaves up to mid-infrared. The efficiency of the frequency upconversion effect in graphene can be increased further by using the plasmon, the cyclotron, or the magnetoplasmon resonances.

The predicted nonlinear phenomena in graphene open up new exciting opportunities for building electronic and optoelectronic devices for the terahertz and subterahertz part of the electromagnetic spectrum.

Acknowledgments

This work was partly supported by the Swedish Research Council and INTAS.

Appendix. Function $\mathcal{G}(Q)$

The function

$$\mathcal{G}(Q) = \frac{4}{\pi Q}\int_0^{\pi/2} \cos\theta \mathrm{d}\theta \left(\sqrt{1+Q\cos\theta} - \sqrt{1-Q\cos\theta}\right) \tag{A.1}$$

can be expanded in powers of Q,

$$\mathcal{G}(Q) = \sum_{l=0}^{\infty} \frac{\Gamma(3/2)}{\Gamma(1/2-2l)} \frac{Q^{2l}}{2^{2l-1} l!(l+1)!}. \tag{A.2}$$

Since $|Q| = |2P/(1+P^2)| \leqslant 1$, expansion (A.2) is valid at all values of P. The first terms of this expansion are

$$\mathcal{G}(Q) \approx 1 + \frac{3}{32}Q^2 + \frac{35}{1024}Q^4 \ldots. \tag{A.3}$$

If $Q = 1$, then

$$\mathcal{G}(1) = \frac{8\sqrt{2}}{3\pi} \approx 1.200. \tag{A.4}$$

The solution of equation (27) can be written as follows:

$$\Gamma t = \int_{P(t)}^{P_0} \frac{\sqrt{1+P^2}}{P\mathcal{G}(Q)}\mathrm{d}P, \qquad Q = \frac{2P}{1+P^2}, \tag{A.5}$$

where $P(t)$ is the projection of the vector $\mathbf{P}(t)$ on the direction of the external electric field and $P_0 \equiv P(0) = eE_0\tau_0/p_{\rm F}$.

References

[1] Sherwin M S, Schmuttenmaer C A and Bucksbaum P H (ed) 2004 Opportunities in THz science *Report of a DOE-NSF-NIH Workshop (Arlington, VA)* http://www.sc.doe.gov/bes/reports/files/THz_rpt.pdf

[2] Faist J, Capasso F, Sivco D L, Sirtori C, Hutchinson A L and Cho A Y 1994 Quantum cascade laser *Science* **264** 553

[3] Siegel P H 2002 Terahertz technology *IEEE Trans. Microw. Theory Tech.* **50** 910

[4] Raisanen A V 1992 Frequency multipliers for millimeter and submillimeter wavelengths *Proc. IEEE* **80** 1842

[5] Mikhailov S A 2007 Non-linear electromagnetic response of graphene *Europhys. Lett.* **79** 27002

[6] Novoselov K S, Geim A K, Morozov S V, Jiang D, Zhang Y, Dubonos S V, Grigorieva I V and Firsov A A 2004 Electric field effect in atomically thin carbon films *Science* **306** 666

[7] Novoselov K S, Geim A K, Morozov S V, Jiang D, Katsnelson M I, Grigorieva I V, Dubonos S V and Firsov A A 2005 Two-dimensional gas of massless Dirac fermions in graphene *Nature* **438** 197

[8] Zhang Y, Tan Y-W, Stormer H L and Kim P 2005 Experimental observation of the quantum Hall effect and Berry's phase in graphene *Nature* **438** 201

[9] Katsnelson M I 2007 Graphene: carbon in two dimensions *Mater. Today* **10** 20

[10] Geim A K and Novoselov K S 2007 The rise of graphene *Nat. Mater.* **6** 183

[11] Wallace P R 1947 The band theory of graphite *Phys. Rev.* **71** 622

[12] Slonczewski J C and Weiss P R 1958 Band structure of graphite *Phys. Rev.* **109** 272

[13] Hasegawa Y, Konno R, Nakano H and Kohmoto M 2006 Zero modes of tight-binding electrons on the honeycomb lattice *Phys. Rev.* B **74** 033413

[14] Semenoff G W 1984 Condensed-matter simulation of a three-dimensional anomaly *Phys. Rev. Lett.* **53** 2449

[15] Katsnelson M I 2006 Zitterbewegung, chirality, and minimal conductivity in graphene *Eur. Phys. J.* B **51** 157

[16] Peres N M R, Guinea F and Castro Neto A H 2006 Electronic properties of disordered two-dimensional carbon *Phys. Rev.* B **73** 125411

[17] Tworzydlo J, Trauzettel B, Titov M, Rycerz A and Beenakker C W J 2006 Sub-Poissonian shot noise in graphene *Phys. Rev. Lett.* **96** 246802

[18] Nomura K and MacDonald A H 2006 Quantum Hall ferromagnetism in graphene *Phys. Rev. Lett.* **96** 256602

[19] Ostrovsky P M, Gornyi I V and Mirlin A D 2006 Electron transport in disordered graphene *Phys. Rev.* B **74** 235443

[20] Ziegler K 2006 Robust transport properties in graphene *Phys. Rev. Lett.* **97** 266802

[21] Cserti J 2007 Minimal longitudinal dc conductivity of perfect bilayer graphene *Phys. Rev.* B **75** 033405

[22] Ryu S, Mudry C, Furusaki A and Ludwig A W W 2007 Landauer conductance and twisted boundary conditions for

Dirac fermions in two space dimensions *Phys. Rev.* B **75** 205344
[23] Nomura K and MacDonald A H 2007 Quantum transport of massless Dirac fermions *Phys. Rev. Lett.* **98** 076602
[24] Ziegler K 2007 Minimal conductivity of graphene: nonuniversal values from the Kubo formula *Phys. Rev.* B **75** 233407
[25] Falkovsky L A and Varlamov A A 2007 Space–time dispersion of graphene conductivity *Eur. Phys. J.* B **56** 281
[26] Cheianov V V, Fal'ko V I, Altshuler B L and Aleiner I L 2007 Random resistor network model of minimal conductivity in graphene *Phys. Rev. Lett.* **99** 176801
[27] Morozov S V, Novoselov K S, Katsnelson M I, Schedin F, Ponomarenko L A, Jiang D and Geim A K 2006 Strong suppression of weak (anti)localization in graphene *Phys. Rev. Lett.* **97** 016801
[28] Gusynin V P and Sharapov S G 2005 Unconventional integer quantum Hall effect in graphene *Phys. Rev. Lett.* **95** 146801
[29] Gusynin V P and Sharapov S G 2006 Transport of Dirac quasiparticles in graphene: Hall and optical conductivities *Phys. Rev.* B **73** 245411
[30] Gusynin V P, Sharapov S G and Carbotte J P 2007 Sum rules for the optical and Hall conductivity in graphene *Phys. Rev.* B **75** 165407
[31] Novoselov K S, Jiang Z, Zhang Y, Morozov S V, Stormer H L, Zeitler U, Maan J C, Boebinger G S, Kim P and Geim A K 2007 Room-temperature quantum Hall effect in graphene *Science* **315** 1379
[32] Sadowski M L, Martinez G, Potemski M, Berger C and de Heer W A 2006 Landau level spectroscopy of ultrathin graphite layers *Phys. Rev. Lett.* **97** 266405
[33] Sadowski M L, Martinez G, Potemski M, Berger C and de Heer W A 2007 Magnetospectroscopy of epitaxial few-layer graphene *Solid State Commun.* **143** 123
[34] Bostwick A, Ohta T, Seyller T, Horn K and Rotenberg E 2007 Quasiparticle dynamics in graphene *Nat. Phys.* **3** 36
[35] Deacon R S, Chuang K-C, Nicholas R J, Novoselov K S and Geim A K 2007 Cyclotron resonance study of the electron and hole velocity in graphene monolayers *Phys. Rev.* B **76** 081406
[36] Jiang Z, Henriksen E A, Tung L C, Wang Y-J, Schwartz M E, Han M Y, Kim P and Stormer H L 2007 Infrared spectroscopy of Landau levels of graphene *Phys. Rev. Lett.* **98** 197403
[37] Henriksen E A, Jiang Z, Tung L C, Schwartz M E, Takita M, Wang Y-J, Kim P and Stormer H L 2008 Cyclotron resonance in bilayer graphene *Phys. Rev. Lett.* **100** 087403
[38] Kuzmenko A B, van Heumen E, Carbone F and van der Marel D 2008 Universal optical conductance of graphite *Phys. Rev. Lett.* **100** 117401
[39] Nair R, Blake P, Grigorenko A, Novoselov K, Booth T, Stauber T, Peres N and Geim A 2008 Universal dynamic conductivity and quantized visible opacity of suspended graphene *Science* doi:10.1126/science.1156965
[40] Nilsson J, Castro Neto A H, Guinea F and Peres N M R 2006 Electronic properties of graphene multilayers *Phys. Rev. Lett.* **97** 266801
[41] Trauzettel B, Blanter Y M and Morpurgo A F 2007 Photon-assisted transport in graphene: scattering theory analysis *Phys. Rev.* B **75** 035305
[42] Gusynin V P, Sharapov S G and Carbotte J P 2006 Unusual microwave response of Dirac quasiparticles in graphene *Phys. Rev. Lett.* **96** 256802
[43] Gusynin V P, Sharapov S G and Carbotte J P 2007 Magneto-optical conductivity in graphene *J. Phys.: Condens. Matter* **19** 026222
[44] Gusynin V P, Sharapov S G and Carbotte J P 2007 Anomalous absorption line in the magneto-optical response of graphene *Phys. Rev. Lett.* **98** 157402
[45] Falkovsky L A and Pershoguba S S 2007 Optical far-infrared properties of a graphene monolayer and multilayer *Phys. Rev.* B **76** 153410
[46] Abergel D S L and Fal'ko V I 2007 Optical and magneto-optical far-infrared properties of bilayer graphene *Phys. Rev.* B **75** 155430
[47] Hwang E H and Das Sarma S 2007 Dielectric function, screening, and plasmons in 2D graphene *Phys. Rev.* B **75** 205418
[48] Wunsch B, Stauber T, Sols F and Guinea F 2006 Dynamical polarization of graphene at finite doping *New J. Phys.* **8** 318
[49] Apalkov V, Wang X-F and Chakraborty T 2007 Collective excitations of Dirac electrons in graphene *Int. J. Mod. Phys.* B **21** 1165
[50] Ryzhii V 2006 Terahertz plasma waves in gated graphene heterostructures *Japan. J. Appl. Phys.* **45** L923
[51] Ryzhii V, Satou A and Otsuji T 2007 Plasma waves in two-dimensional electron–hole system in gated graphene heterostructures *J. Appl. Phys.* **101** 024509
[52] Vafek O 2006 Thermoplasma polariton within scaling theory of single-layer graphene *Phys. Rev. Lett.* **97** 266406
[53] Mikhailov S A and Ziegler K 2007 New electromagnetic mode in graphene *Phys. Rev. Lett.* **99** 016803
[54] Mikhailov S A 2008 Electromagnetic response of electrons in graphene: non-linear effects *Physica* E **40** 2626–9
[55] Dyakonov M and Shur M 1993 Shallow water analogy for a ballistic field effect transistor: new mechanism of plasma wave generation by dc current *Phys. Rev. Lett.* **71** 2465
[56] Dyakonov M and Shur M S 2001 *Terahertz Sources and Systems* (*NATO Science Series II. Mathematics, Physics and Chemistry* vol 27) ed R E Miles, P Harrison and D Lippens (Dordrecht: Kluwer) pp 187–207
[57] Shur M S and Ryzhii V 2003 Plasma wave electronics *Int. J. High Speed Electron. Syst.* **13** 575
[58] Mikhailov S A 1998 Plasma instability and amplification of electromagnetic waves in low-dimensional electron systems *Phys. Rev.* B **58** 1517
[59] Kukushkin I V, Akimov M Y, Smet J H, Mikhailov S A, von Klitzing K, Aleiner I L and Falko V I 2004 New type of B-periodic magneto-oscillations in a two-dimensional electron system induced by microwave irradiation *Phys. Rev. Lett.* **92** 236803
[60] Mikhailov S, Kukushkin I, Smet J and von Klitzing K 2004 *Passive Millimetre-Wave and Terahertz Imaging and Technology*; *Proc. SPIE* **5619** 187–97
[61] Tsui D C, Gornik E and Logan R A 1980 Far infrared emission from plasma oscillations of Si inversion layers *Solid State Commun.* **35** 875
[62] Hirakawa K, Yamanaka K, Grayson M and Tsui D C 1995 Far-infrared emission spectroscopy of hot two-dimensional plasmons in $Al_{0.3}Ga_{0.7}As$/GaAs heterojunctions *Appl. Phys. Lett.* **67** 2326
[63] Knap W, Deng Y, Rumyantsev S and Shur M S 2002 Resonant detection of subterahertz and terahertz radiation by plasma waves in submicron field-effect transistors *Appl. Phys. Lett.* **81** 4637
[64] Kukushkin I V, Mikhailov S A, Smet J H and von Klitzing K 2005 Miniature quantum-well microwave spectrometer operating at liquid-nitrogen temperatures *Appl. Phys. Lett.* **86** 044101
[65] Slepyan G Y, Maksimenko S A, Kalosha V P, Herrmann J, Campbell E E B and Hertel I V 1999 Highly efficient high-order harmonic generation by metallic carbon nanotubes *Phys. Rev.* A **60** R777
[66] Stanciu C *et al* 2002 Experimental and theoretical study of third-order harmonic generation in carbon nanotubes *Appl. Phys. Lett.* **81** 4064
[67] Kibis O V, Parfitt D G W and Portnoi M E 2005 Superlattice properties of carbon nanotubes in a transverse electric field *Phys. Rev.* B **71** 035411

[68] Kibis O V and Portnoi M E 2005 Carbon nanotubes: a new type of emitter in the terahertz range *Tech. Phys. Lett.* **31** 671
[69] Nemilentsau A M, Slepyan G Y, Khrutchinskii A A and Maksimenko S A 2006 Third-order optical nonlinearity in single-wall carbon nanotubes *Carbon* **44** 2246
[70] Kuzhir P P, Batrakov K G and Maksimenko S A 2007 Generation and propagation of electromagnetic waves in carbon nanotubes: new propositon for optoelectronics and bio-medical applications *Synth. React. Inorg. Met.-Org. Nano-Met. Chem.* **37** 341
[71] Kibis O V, da Costa M R and Portnoi M E 2007 Generation of terahertz radiation by hot electrons in carbon nanotubes *Nano Lett.* **7** 3414
[72] Portnoi M E, Kibis O V and da Costa M R 2008 Terahertz applications of carbon nanotubes *Superlatt. Microstruct.* **43** 399–407
[73] Martin J, Akerman N, Ulbricht G, Lohmann T, Smet J H, von Klitzing K and Yacoby A 2008 Observation of electron–hole puddles in graphene using a scanning single-electron transistor *Nat. Phys.* **4** 144
[74] Mikhailov S A 2004 Microwave-induced magnetotransport phenomena in two-dimensional electron systems: importance of electrodynamic effects *Phys. Rev.* B **70** 165311
[75] Mikhailov S A 1996 Radiative decay of collective excitations in an array of quantum dots *Phys. Rev.* B **54** 10335